JOURNAL OF Applied Polymer SCIENCE

Special Issue: Microfiltration and Ultrafiltration Membrane Science and Technology

Guest Editors: Prof. Isabel C. Escobar (University of Toledo) and Prof. Bart Van der Bruggen (University of Leuven)

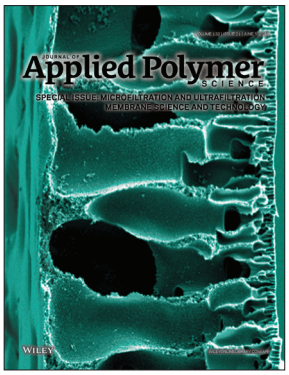

EDITORIAL

Microfiltration and Ultrafiltration Membrane Science and Technology
I. C. Escobar and B. Van der Bruggen, *J. Appl. Polym. Sci.* 2015, **DOI: 10.1002/app.42002**

REVIEWS

Nanoporous membranes generated from self-assembled block polymer precursors: *Quo Vadis*?
Y. Zhang, J. L. Sargent, B. W. Boudouris and W. A. Phillip, *J. Appl. Polym. Sci.* 2015, **DOI: 10.1002/app.41683**

Making polymeric membranes anti-fouling via "grafting from" polymerization of zwitterions
Q. Li, J. Imbrogno, G. Belfort and X.-L. Wang, *J. Appl. Polym. Sci.* 2015, **DOI: 10.1002/app.41781**

Fouling control on MF/ UF membranes: Effect of morphology, hydrophilicity and charge
R. Kumar and A. F. Ismail, *J. Appl. Polym. Sci.* 2015, **DOI: 10.1002/app.42042**

EMERGING MATERIALS AND FABRICATION

Preparation of a poly(phthalazine ether sulfone ketone) membrane with propanedioic acid as an additive and the prediction of its structure
P. Qin, A. Liu and C. Chen, *J. Appl. Polym. Sci.* 2015, **DOI: 10.1002/app.41621**

Preparation and characterization of MOF-PES ultrafiltration membranes
L. Zhai, G. Li, Y. Xu, M. Xiao, S. Wang and Y. Meng, *J. Appl. Polym. Sci.* 2015, **DOI: 10.1002/app.41663**

Tailoring of structures and permeation properties of asymmetric nanocomposite cellulose acetate/silver membranes
A. S. Figueiredo, M. G. Sánchez-Loredo, A. Maurício, M. F. C. Pereira, M. Minhalma and M. N. de Pinho, *J. Appl. Polym. Sci.* 2015, **DOI: 10.1002/app.41796**

LOW-FOULING POLYMERS

Low fouling polysulfone ultrafiltration membrane via click chemistry
Y. Xie, R. Tayouo and S. P. Nunes, *J. Appl. Polym. Sci.* 2015, **DOI: 10.1002/app.41549**

Elucidating membrane surface properties for preventing fouling of bioreactor membranes by surfactin
N. Behary, D. Lecouturier, A. Perwuelz and P. Dhulster, *J. Appl. Polym. Sci.* 2015, **DOI: 10.1002/app.41622**

PVC and PES-*g*-PEGMA blend membranes with improved ultrafiltration performance and fouling resistance
S. Jiang, J. Wang, J. Wu and Y. Chen, *J. Appl. Polym. Sci.* 2015, **DOI: 10.1002/app.41726**

Improved antifouling properties of TiO_2/PVDF nanocomposite membranes in UV coupled ultrafiltration
M. T. Moghadam, G. Lesage, T. Mohammadi, J.-P. Mericq, J. Mendret, M. Heran, C. Faur, S. Brosillon, M. Hemmati and F. Naeimpoor, *J. Appl. Polym. Sci.* 2015, **DOI: 10.1002/app.41731**

Development of functionalized doped carbon nanotube/polysulfone nanofiltration membranes for fouling control
P. Xie, Y. Li and J. Qiu, *J. Appl. Polym. Sci.* 2015, **DOI: 10.1002/app.41835**

JOURNAL OF Applied Polymer SCIENCE

Special Issue: Microfiltration and Ultrafiltration Membrane Science and Technology

Guest Editors: Prof. Isabel C. Escobar (University of Toledo) and
Prof. Bart Van der Bruggen (University of Leuven)

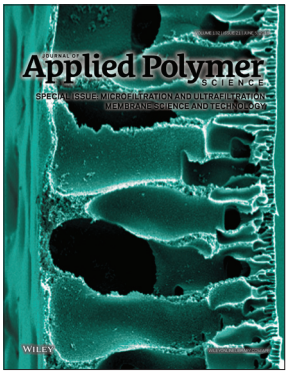

SURFACE MODIFICATION OF POLYMER MEMBRANES

Highly chlorine and oily fouling tolerant membrane surface modifications by *in situ* polymerization of dopamine and poly(ethylene glycol) diacrylate for water treatment
K. Yokwana, N. Gumbi, F. Adams, S. Mhlanga, E. Nxumalo and B. Mamba, *J. Appl. Polym. Sci.* 2015, **DOI: 10.1002/app.41661**

Fouling control through the hydrophilic surface modification of poly(vinylidene fluoride) membranes
H. Jang, D.-H. Song, I.-C. Kim, and Y.-N. Kwon, *J. Appl. Polym. Sci.* 2015, **DOI: 10.1002/app.41712**

Hydroxyl functionalized PVDF-TiO_2 ultrafiltration membrane and its antifouling properties
Y. H. Teow, A. A. Latif, J. K. Lim, H. P. Ngang, L. Y. Susan and B. S. Ooi, *J. Appl. Polym. Sci.* 2015, **DOI: 10.1002/app.41844**

Enhancing the antifouling properties of polysulfone ultrafiltration membranes by the grafting of poly(ethylene glycol) derivatives via surface amidation reactions
H. Yu, Y. Cao, G. Kang, Z. Liu, W. Kuang, J. Liu and M. Zhou, *J. Appl. Polym. Sci.* 2015, **DOI: 10.1002/app.41870**

SEPARATION APPLICATIONS

Experiment and simulation of the simultaneous removal of organic and inorganic contaminants by micellar enhanced ultrafiltration with mixed micelles
A. D. Vibhandik, S. Pawar and K. V. Marathe, *J. Appl. Polym. Sci.* 2015, **DOI: 10.1002/app.41435**

Polymeric membrane modification using SPEEK and bentonite for ultrafiltration of dairy wastewater
A. Pagidi, Y. Lukka Thuyavan, G. Arthanareeswaran, A. F. Ismail, J. Jaafar and D. Paul, *J. Appl. Polym. Sci.* 2015, **DOI: 10.1002/app.41651**

Forensic analysis of degraded polypropylene hollow fibers utilized in microfiltration
X. Lu, P. Shah, S. Maruf, S. Ortiz, T. Hoffard and J. Pellegrino, *J. Appl. Polym. Sci.* 2015, **DOI: 10.1002/app.41553**

A surface-renewal model for constant flux cross-flow microfiltration
S. Jiang and S. G. Chatterjee, *J. Appl. Polym. Sci.* 2015, **DOI: 10.1002/app.41778**

Ultrafiltration of aquatic humic substances through magnetically responsive polysulfone membranes
N. A. Azmi, Q. H. Ng and S. C. Low, *J. Appl. Polym. Sci.* 2015, **DOI: 10.1002/app.41874**

BIOSEPARATIONS APPLICATIONS

Analysis of the effects of electrostatic interactions on protein transport through zwitterionic ultrafiltration membranes using protein charge ladders
M. Hadidi and A. L. Zydney, *J. Appl. Polym. Sci.* 2015, **DOI: 10.1002/app.41540**

Modification of microfiltration membranes by hydrogel impregnation for pDNA purification
P. H. Castilho, T. R. Correia, M. T. Pessoa de Amorim, I. C. Escobar, J. A. Queiroz, I. J. Correia and A. M. Morão, *J. Appl. Polym. Sci.* 2015, **DOI: 10.1002/app.41610**

Hemodialysis membrane surface chemistry as a barrier to lipopolysaccharide transfer
B. Madsen, D. W. Britt, C.-H. Ho, M. Henrie, C. Ford, E. Stroup, B. Maltby, D. Olmstead and M. Andersen, *J. Appl. Polym. Sci.* 2015, **DOI: 10.1002/app.41550**

Membrane adsorbers comprising grafted glycopolymers for targeted lectin binding
H. C. S. Chenette and S. M. Husson, *J. Appl. Polym. Sci.* 2015, **DOI: 10.1002/app.41437**

Journal of Applied Polymer Science

Experiment and simulation of the simultaneous removal of organic and inorganic contaminants by micellar enhanced ultrafiltration with mixed micelles

Amar D. Vibhandik, Snehal Pawar, Kumudini V. Marathe
Department of Chemical Engineering, Institute of Chemical Technology, Matunga 400019, Mumbai
Correspondence to: K. V. Marathe (E-mail: kv.marathe@ictmumbai.edu.in)

ABSTRACT: Lead, chromium, and chlorobenzene (CB) were removed simultaneously by micellar enhanced ultrafiltration with a mixture of anionic and nonionic surfactants. The process parameters, including the molar ratio of the nonionic surfactant to the ionic surfactant (α), surfactant to metal ion (S/M) molar ratio, applied pressure, and inlet flow rate, were investigated. As α was varied from 0 to 1.5, the rejection of the metal ions increased. The optimum α value was 0.5. The permeate flux decreased by 28% with increasing α from 0 to 1.5. The S/M ratio was optimized at 10 in the presence of CB. The addition of CB increased the rejection of surfactants and decreased the metal-ion rejection. The effect of the applied pressure and inlet flow were studied and found to be optimum at 1 bar and 150 mL/min, respectively. The optimized parameters were applied to the steady-state process. The multiple-solute model was applied to the steady-state data. The relative error for solute rejection was varied from 5 to 9%, and the relative error for flux was 5%. © 2014 Wiley Periodicals, Inc. J. Appl. Polym. Sci. **2015**, *132*, 41435.

KEYWORDS: membranes; micelles; separation techniques; surfactants

Received 30 May 2014; accepted 25 August 2014
DOI: 10.1002/app.41435

INTRODUCTION

Potable water is quite often polluted by civil and industrial wastewater; this results in its scarcity. Civil wastewater contains mainly commodity chemicals, metal ions, edible oil traces, and biological wastes. Industry waste contains heavy-metal ions of copper, chromium, nickel, zinc, lead, and so on, and organic solvents such as chlorobenzene (CB), tetrachloroethylene, trichloroethylene, methylene chloride, 1,1,1-trichloroethane, carbon tetrachloride, and paints.[1] Conventional processes, such as chemical precipitation, extraction, and distillation, are used to treat industry wastewater. However, these methods have their own disadvantages and seem to be economically unfeasible;[2] hence, it is essential to find a better alternative. Membrane separation will be a good alternative for the treatment of industrial wastewater. Reverse osmosis and nanofiltration can be directly applied to treat wastewater for the removal of heavy-metal ions. However, these processes are highly energy intensive and have a high capital cost.[3] The surfactant has the characteristic of forming micelles above a particular concentration called the *critical micelle concentration* (cmc). The micelle has an inner core that is hydrophobic, and its surface is hydrophilic. Metal ions bind to the micelle, and organic compounds go inside the micelle. The micelle is bigger than the ultrafiltration (UF) membrane; hence, it is rejected by the membrane in the ultrafiltration process.[4] Thus, micellar-enhanced ultrafiltration (MEUF) combines the advantages of both a high flux and a high rejection rate.

Huang *et al.*[5] removed divalent metal ions, such as lead, cadmium, copper, nickel, and zinc, individually and simultaneously with deoxycholic acid, lecithin, and sodium dodecyl sulfate (SDS). They concluded that the optimum surfactant to metal ion (S/M) molar ratios for SDS and deoxycholic acid were 5 and 3, respectively.

Generally, anionic surfactants possess higher cmc values than cationic and nonionic surfactants. It was found that a surfactant with the higher cmc needs a greater amount of surfactant for proper micellization and better rejection by MEUF. This may also result in a high surfactant concentration in the permeate stream. Hence, there is a need to decrease the cmc of anionic surfactants. Most nonionic surfactants, except glucose-based surfactants, have oxyethylene chains, which act as hydrophilic heads, and alkyl chains, which act as hydrophobic tails of the surfactant. The polyoxyethylene head shows less repulsion than other surfactant heads. Hence, nonionic surfactants show lower cmc's than anionic surfactants.[6] The addition of a nonionic surfactant to an anionic surfactant solution reduces the cmc of a mixture. Huang *et al.*[7] removed Cd^{2+} ions with surfactant pairs, including SDS–Brij 35 and SDS–Triton X-100 (TX-100). Aoudia

Table I. Properties of the Membrane and Surfactants

Surfactant	Structure	Molecular weight cutoff/ molecular weight (Da)	cmc (mM)
PES	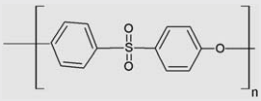	10,000	—
SDS	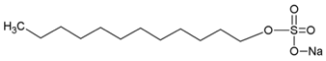	288	8
Tween 80	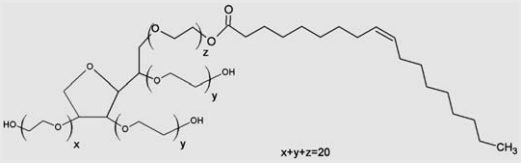	1310	0.04

et al.[8] removed chromium(III) with an SDS–nonyl phenol ethoxylate pair. Huang *et al.*[9] simultaneously separated methylene blue dye and Cd^{2+} from aqueous waste. Lee *et al.*[10] simultaneously extracted chromate ions and trichloroethylene with cetyl pyridinum chloride (CPC) and Tween 80 (TW80). Li *et al.*[11] separated cadmium ions and phenol with an SDS–TX100 system. Yenphan *et al.*[12] separated lead ions from wastewater with the surfactant mixtures SDS–TX100 and SDS–NP12. Zhao *et al.*[13] worked on the removal of CB and nickel ions and optimized the α, pH, and pressure values. Thus, literature available on the SDS–TW80 surfactant pair is scarce.

The resistance in a series model based on Darcy's law was investigated; it was based on the dependence of the flux on the pressure gradient and viscosity (μ).[14–17] A general membrane-fouling model that accounted for the internal clogging, partial and total clogging, cake deposition, and cake deposition with retro flux for an ultrafiltration system was developed by Ghaffour.[18] Damak *et al.*[19] developed a fluid dynamic model for the cross-flow filtration of tubular membranes. Katsikaris *et al.*[20] developed a mathematical model for the simulation of an ultrafiltration system; it accounted for the concentration polarization phenomena on the basis of thin film theory. Ahmad *et al.*[21] worked on Palm Oil Mill Effluent (POME) waste and also modeled the flux and concentration of each solute with time.

The objective of this study was to examine the effectiveness of MEUF for complex synthetic wastewater containing Pb, Cr, and CB and to optimize the process parameters and its application to steady-state processes. Another objective was the simulation of the experimental results and the validation of the model with steady-state data.

EXPERIMENTAL

Chemicals

All of the reagents were analytical grade. SDS was procured from Merck India Pvt., Ltd. (Mumbai, India). Lead nitrate [$Pb(NO_3)_2{\cdot}7H_2O$, 98% pure], chromium chloride ($CrCl_3{\cdot}6H_2O$, 99% pure), and polyoxyethylene (20) sorbitan monooleate (TW80) were obtained from S. D. Fine Chemicals, Ltd. (Mumbai, India). The properties of the surfactants are given in Table I. All of the samples for the experiments were prepared in deionized (DI) water (conductivity = 0.05 μS/cm).

Membranes

A flat-sheet membrane made up of poly(ether sulfone) (PES) material was used. The membrane was hydrophilic in nature. The details about the membrane are given in Table I. The membrane was supplied by Hydronautics Nitto Denko Co., India.

Experimental Setup and Method

Figure 1 shows the schematic experimental setup. The membrane holder was fabricated in house and was made up of polytetrafluoroethylene. The effective area for filtration was 21.53 cm^2. A peristaltic pump having a maximum sustainable pressure of 6 bars was used to pressurize the system. The membrane was cleaned by DI water at a high inlet flow rate and zero pressure.

In each experimental run, all of the samples were prepared by DI water. The applied pressure and flow rate were taken as 25 kPa and 100 mL/min, respectively, for the optimization of α and the S/M ratio. In these experiments, the permeate and retentate were recycled to the feed tank to maintain a constant feed concentration. All of the experiments were performed at room temperature (~28°C). The samples for each experiment were taken after 30 min to achieve the equilibrium state.

The removal efficiency of the solutes or the pollutant (%R) was calculated by the following equation:

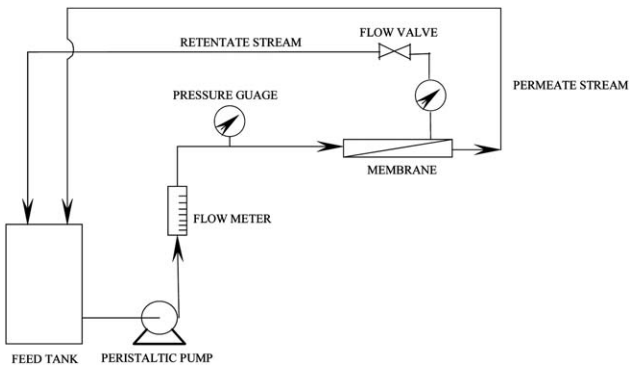

Figure 1. Schematic of the experimental setup.

$$\%R=\left(1-\frac{C_p}{C_b}\right)\times 100 \quad (1)$$

where C_{pi} is the concentration of species 'i' in permeate stream (kmol/m^3) and C_b is the concentration of the pollutant in the feed tank (kmol/m^3). The permeate flux was calculated by the following equation:

$$J=\frac{V}{tA} \quad (2)$$

where J is the absolute permeate flux (m^3 m^{-2} s^{-1}), V is the volume of the permeate sample collected (m^3), t is the time needed (s) to collect the permeate volume (V_p), and A is the membrane effective area. In addition, the relative flux was calculated as the ratio of the absolute flux to the pure water flux obtained under identical experimental conditions.

Measurement and Analysis

The concentration of SDS was measured by the methylene blue spectrophotometric method.[22] The concentration of SDS was determined at a wavelength of 652 nm. An inductively coupled plasma spectrophotometer (i-Cap 6000, Thermo-Fisher India) was used for the detection of chromium and lead ions. The UV-2700 Chemito ultraviolet–visible spectrophotometer was used for all of the previous spectrophotometric detections. High-pressure liquid chromatography (HPLC) method was used for the detection of TW80 and CB. The HPLC instrument (Thermo Scientific) was operated at a 1 mL/min flow rate with a mobile phase of acetonitrile/water (85/15 v/v) at UV wavelengths of 232 and 254 nm for TW80 and CB, respectively. A C18 symmetry column (Knauer) was used for the operation.

THEORY OF SIMULATION

Multiple-Solute Model

In the cross-flow ultrafiltration of the multiple-solute system, the following assumptions were made:

1. The membrane rejected the multiple solutes by a sieving action, and the membrane–solute and solute–solute interactions were neglected.

2. Because the membrane–solute and solute–solute interactions were neglected, the concentration of each solute was obtained by mass balance analysis with the consideration of the back-transport effect.

3. In the gel layer, each solute will have its independent value of diffusion, mass-transfer and back-transport coefficient.[21,23]

For the simplicity of the model, the mass balance in the boundary layer was ignored, with the assumption that the total mass of the solute obtained in the boundary layer was negligible compared to total mass of the solute obtained in the gel layer.

The mass of the total solutes in the gel layer at any filtration time (t) was

$$V_g C_g=(V_p+V_g)C_b-V_pC_p-M_{bt} \quad (3)$$

where C_b as bulk feed concentration (C_b), V_g is the volume of gel layer in m^3, C_g gel layer concentration in kmol/m^3, and M_{bt} is the bulk mass transport rate in kmol/second. The total mass balance of the system was the sum of the mass balance of the individual solutes. Therefore, eq. (1) can be written as follows:

$$V_g\sum_{i=1}^{n}C_{gi}=(V_p+V_g)\sum_{i=1}^{n}C_{bi}-V_p\sum_{i=1}^{n}C_{pi}-\sum_{i=1}^{n}M_{bti} \quad (4)$$

where C_{gi} is the concentration of each solute in the gel layer, C_{bi} is the bulk concentration of each solute, C_{pi} is the permeate concentration of each solute, and M_{bti} is the back-transport mass of each solute.

M_{bti} is given by

$$M_{bti}=K_{bi}vC_{gi} \quad (5)$$

where K_{bi} is the back-transport coefficient of each solute and v is the superficial velocity.

The total volume flux of the permeate (J_p) could be calculated with the osmotic pressure model:[23,24]

$$J_p=\frac{1}{A_m}\frac{dV_p}{dt}=\frac{\Delta P-\Delta\pi}{\mu(R_H)} \quad (6)$$

where A_m is the membrane area; ΔP, or TMP, is the transmembrane pressure; $\Delta\pi$ is the osmotic pressure difference; and R_H is the total hydraulic resistance (m^{-1}), which is the sum of the membrane resistance (R_m; m^{-1}) and resistance due to the gel layer (R_g; m^{-1}). J_p can also be calculated with Darcy's law. When these equations are combined, a final equation for resistance in a series model can be obtained to calculate the volume flux of the permeate as

$$\frac{1}{J_p}=a_1+a_2V_p-a_3t \quad (7)$$

where the coefficients a_1, a_2, and a_3 are given by

$$a_1=\frac{\mu R_m}{(\Delta P-\Delta\pi)} \quad (8)$$

$$a_2=\frac{\mu}{A_mP_m(\Delta P-\Delta\pi)}\frac{\sum_{i=1}^{n}(C_{bi}-C_{pi})}{\sum_{i=1}^{n}(C_{gi}-C_{bi})} \quad (9)$$

where P_m is the permeability coefficient. In addition

$$a_3=\frac{\mu v}{A_mP_m(\Delta P-\Delta\pi)}\frac{\sum_{i=1}^{n}K_{bi}\ C_{gi}}{\sum_{i=1}^{n}(C_{gi}-C_{bi})} \quad (10)$$

C_{gi} is calculated by[25]

$$\frac{(C_{gi}-C_{pi})}{(C_{bi}-C_{pi})}=\exp\left(\frac{J_{vss}}{k_i}\right) \quad (11)$$

where k_i is the mass-transfer coefficient, and J_{vss} is the Permeate flux at steady state in m^3.m^{-2}.s^{-1}. C_{pi} is calculated by[21]

$$C_{pi}=C_{bi}-\frac{K_{bi}vC_{gi}}{AJ_{vss}} \quad (12)$$

Determination of the Model Parameters

The multiple-solute model is characterized by operating parameters, such as TMP, v, C_b, and C_{bi} and membrane parameters, such as R_m, $\Delta\pi$, P_m, μ, k_i, and K_{bi}. The model parameters for the simultaneous removal of CB (C_6H_5Cl), Pb(II), and Cr(III) with the mixed surfactants SDS and TW80 were determined with experimental data. R_m was estimated from the slope of a plot of the DI water flux versus $\Delta P/\mu$.

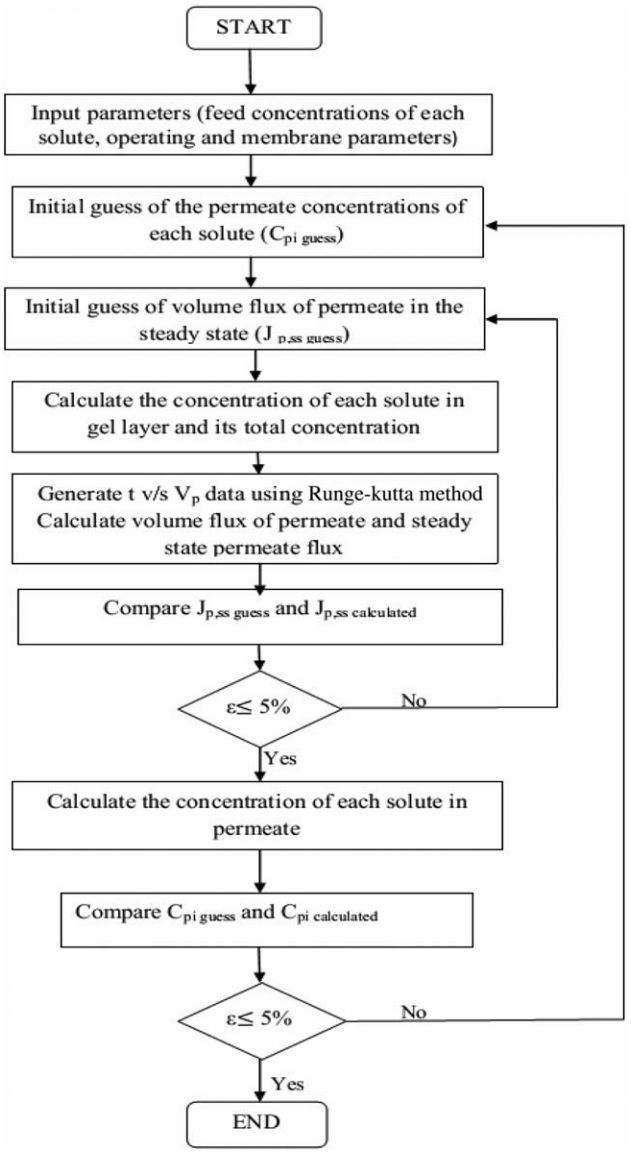

Figure 2. Algorithm of simulation.

C_{gi} was determined by the mass balance with the gel polarization model. K_{bi} was determined from the slope of the graph of C_{pi} versus $vC_{gi}/A_mJ_{p,ss}$ (where $J_{p,ss}$ is the steady-state permeate flux), with the intercept kept constant at C_{bi}.[23]

The simulation procedure is shown in Figure 2. Input to the model, such as the initial feed condition and membrane parameters, were provided with guess values. V_p could be obtained by the integration of eq. (7) with a higher order Runge–Kutta method[26] at equispaced time intervals. The gel layer concentration of the solutes was obtained with eq. (11). The permeate flux became constant over a period of time attaining a steady state. This permeate flux was called $J_{p,ss}$. The C_{pi} values were calculated with eq. (12). The concentration of each solute in the permeate was calculated only when the error in the predicted and guess values of $J_{p,ss}$ were less than or equal to 5%. The calculation procedure was terminated when the error in the guess value of the solute concentration in the permeate and the predicted value was less than or equal to 5%.

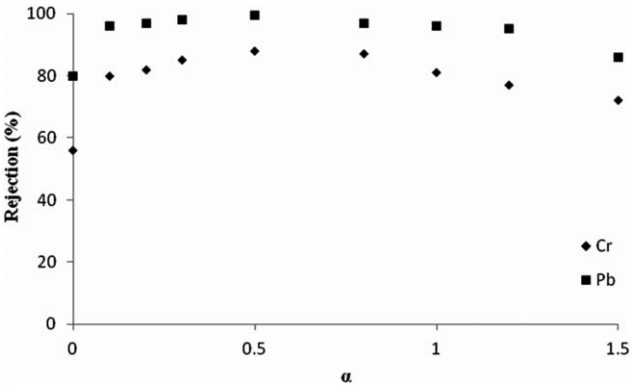

Figure 3. Effect of α on the rejection of solutes.

RESULTS AND DISCUSSION

Effect of the Nonionic Surfactant to Ionic Surfactant Molar Ratios (α) on the Rejection and Permeate Fluxes

The ultrafiltration experiments were done to estimate the effect of α on the rejection of the solutes and the permeate flux. The experiments for chromium and lead ions were carried out individually at a TMP of 25kPa and an inlet velocity of 100 mL/min. The metal-ion concentration was 0.5 m*M*, and the total surfactant concentration was 4 m*M*. The results are shown in Figure 3. At a zero α value, that is, for the pure SDS surfactant, the rejections of the Cr and Pb ions were 57 and 75%, respectively. This was attributed to the concentration polarization and led to gel layer formation or to a drop in the cmc of SDS in the presence of metal salts. This may also have been due to the entrapment of metal ions in the gel layer formed on the membrane surface. Now, at a 0.1 value of α, the rejections of chromium and lead were 80 and 96%, respectively. This showed that the small addition of the TW80 surfactant led to a sharp increase in the rejection of the metal ions. The rejection of the metal ions increased up to a 0.5 value of α and decreased with further increases in α. The rejections of the metal ions at a 1.5 value of α was found to be 86 and 72% for lead and chromium, respectively. The addition of TW80 to the SDS surfactant solution decreased the cmc of mixture and increased the number of

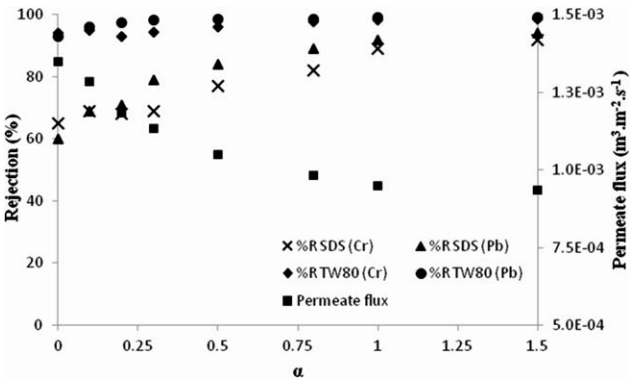

Figure 4. Effect of α on the rejection of the surfactants and the permeate flux of the solute.

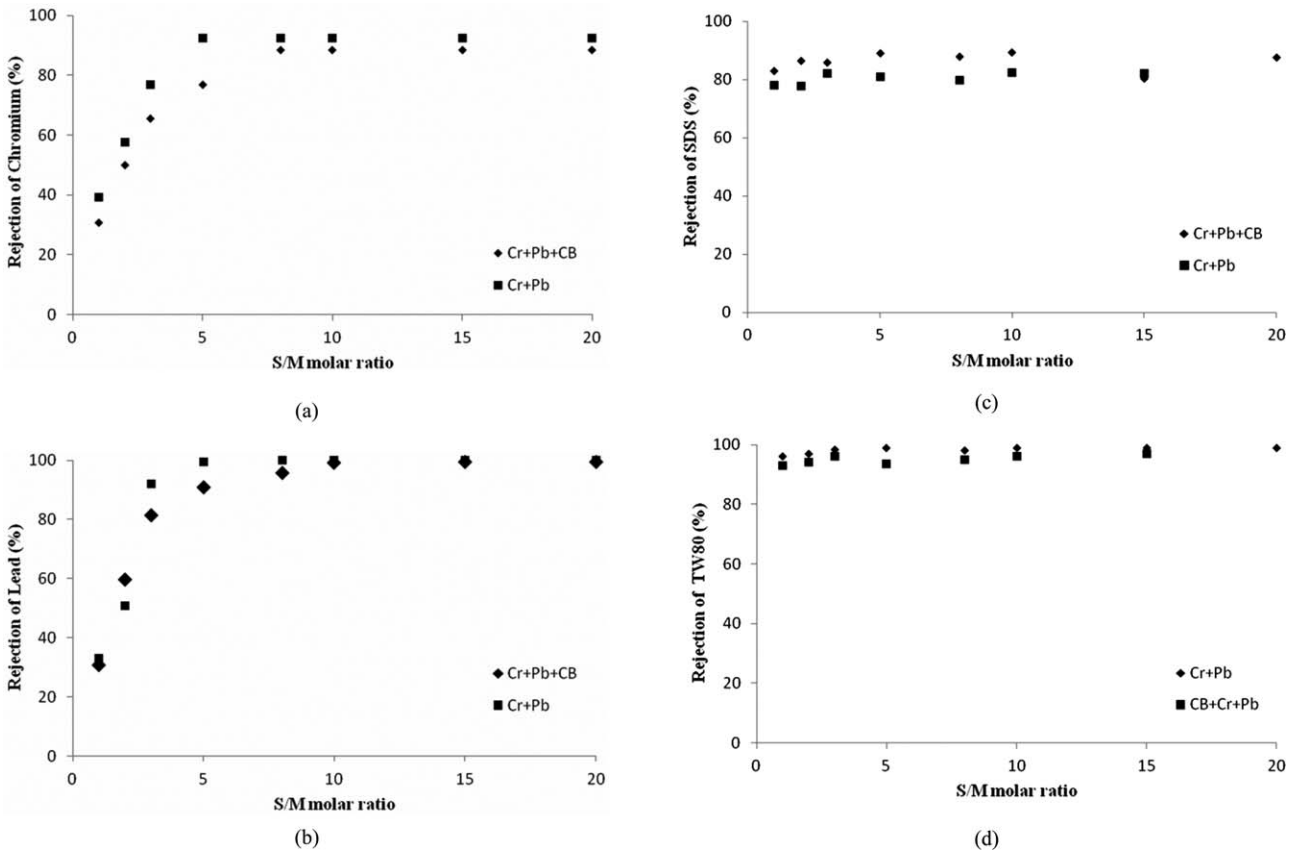

Figure 5. Effect of the S/M ratio on the rejection of (a) Cr, (b) Pb, (c) SDS, and (d) TW80.

micelles in the solution. This indicated an increase in the micelle loading, which increased the metal-ion rejection. A further increase in the TW80 surfactant in the mixture decreased the surface charge density of the micelle; hence, fewer metal ions adsorbed on the micelle. This led to a decrease in the rejection of metal ions. These results were in agreement with Auodia *et al.*,[8] Fang *et al.*,[27] and Huang *et al.*,[9] Figure 4. The rejection of TW80 was constant at 97%, whereas there was an increase in the rejection of SDS with increasing α. An increase in SDS rejection was observed from 62 to 92% as α varied from 0.1 to 1.5, respectively. The decrease in the relative flux was observed with increasing α. The flux decreased by 27% as α varied from 0 to 1.5. This may have been due to the formation of a dense gel layer on the membrane surface with the addition of the TW80 surfactant. Thus, α was empirically optimized at 0.5.

Effect of the Total Surfactant Concentration on the Rejection of the Solutes

The dependence of the solute rejection and permeate flux on the total surfactant concentration at the optimum value of α was investigated, and the data are shown in Figure 5(a–d). The initial chromium and lead ion concentrations in the feed were 0.5 m*M* each. As shown in Figure 5(a), the rejection of chromium at a 1 m*M* total surfactant concentration without CB was 40%, and it rose with the addition of surfactant. At an S/M

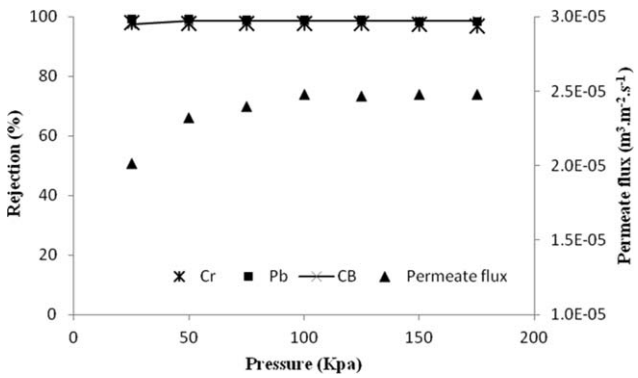

Figure 6. Effect of TMP on the rejection and permeate flux of the solute.

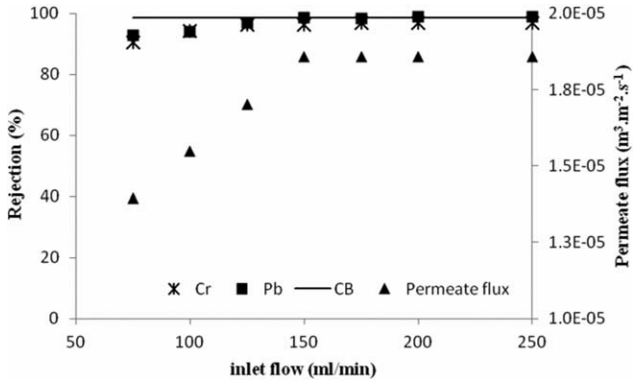

Figure 7. Effect of the inlet flow on the rejection and permeate flux of the solute.

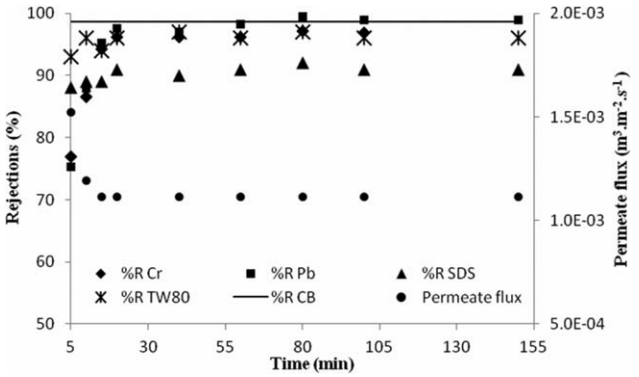

Figure 8. Effect of the operation time on the rejection of the solutes and solvent flux.

ratio of 5, the rejection was 92% and increased up to 99% at S/M ratio = 7 and remained constant further. According to Figure 5(b), lead-ion rejection without CB was 32%, and it increased sharply with increasing S/M ratio. The maximum rejection of lead was obtained as 99.5% at an S/M ratio was 5 and remained constant with the further addition of surfactant. These results were in line with the experimental findings of Auodia *et al.*,[8] Huang *et al.*,[9] Yenphan *et al.*,[12] and Vibhandik and Marathe.[28] The addition of CB was done to check the effect of organics on the rejection of the solutes. The CB concentration was 300 ppm up to its solubility limit at 28°C. According to Figure 5(a,b), we observed that the addition of CB decreased the with respect to (w.r.t.) rejection of metal ions without the addition of CB at respective S/M ratios. This may have been due to the accumulation of CB in the palisade layer and core of the micelle. Initially, without the addition of CB, metal ions may have accumulated in the palisade layer. After the addition of CB, there was no space for metal ions in the palisade layer to accumulate; hence, this lowered the rejection of metal ions.

Figure 5(c) shows the rejection of SDS with respect to the S/M ratio. The rejection of SDS increased from 75 to 83% with increasing S/M ratio from 1 to 15. Furthermore, the SDS rejection increased with the addition of CB by about 5–10%. The rejection of TW80 was observed to be constant at 95% over the entire range of S/M ratios, as shown in Figure 5(d).There was a marginal increase in the rejection of TW80 in the presence of CB. This may have been due to the decrease in the cmc of the surfactant mixture in the presence of CB. This led to an increase in the micellization of more surfactant monomers and resulted in a higher rejection. The S/M molar ratio was optimized at 10.

Table II. Feed Stream Conditions

Parameter	Abbreviation	Value
Transmembrane pressure	ΔP	100,000
Membrane area	A_m	21.5×10^{-4}
Superficial velocity	v	0.00116
Total bulk concentration	C_b	6.71 (13.8)
Feed concentration of Pb(II)	C_{b1}	0.103 (0.5)
Feed concentration of Cr(III)	C_{b2}	0.026 (0.5)
Feed concentration of CB	C_{b3}	0.300 (2.6)
Feed concentration of SDS	C_{b4}	1.92 (6)
Feed concentration of TW80	C_{b5}	4.35 (3.32)

Table III. Operating and Membrane Parameters

Parameter	Notation	Value
Membrane resistance	R_m	1.00×10^{12}
Osmotic pressure difference	$\Delta\pi$	8.16×10^{4}
Permeability coefficient	P_m	$7.14 \times 10^{-}7$
Viscosity	μ	$9.50 \times 10^{-}4$
Mass-transfer coefficient for Pb(II)	k_1	$1.25 \times 10^{-}5$
Mass-transfer coefficient for Cr(III)	k_2	$1.19 \times 10^{-}5$
Mass-transfer coefficient for CB	k_3	$2.74 \times 10^{-}5$
Mass-transfer coefficient for SDS	k_4	$2.56 \times 10^{-}5$
Mass-transfer coefficient for TW80	k_5	$7.52 \times 10^{-}5$
Back-transport coefficient for Pb(II)	K_{b1}	$8.30 \times 10^{-}6$
Back-transport coefficient for Cr(III)	K_{b2}	$8.00 \times 10^{-}6$
Back-transport coefficient for CB	K_{b3}	$20.0 \times 10^{-}6$
Back-transport coefficient for SDS	K_{b4}	$20.0 \times 10^{-}6$
Back-transport coefficient for TW80	K_{b5}	$30.0 \times 10^{-}6$

Effect of the TMP

The effects of TMP on the rejection of the solutes and the permeate flux were observed by MEUF experiments at the optimized α and S/M ratio. The results are depicted in Figure 6. As shown in figure, the permeate flux increased from 2×10^{-5} to 2.4×10^{-5} m^3 m^{-2} s^{-1} as the pressure was varied from 25 to 100 kPa and remained constant with further increases in TMP. Because of the pressure gradient between the two sides of the membrane, the solution was transported toward the membrane and was rejected on the membrane surface. This resulted in the formation of the gel layer. Thus, the gel layer had a high concentration of solutes that was transported back to the bulk stream. At 100 kPa, the convective flux of the solute was counterbalanced by back-transport flux; hence, the permeate flux was observed to be constant.[29] The rejection of solutes was observed to be constant over the entire range of TMPs. The TMP was optimized at 100 kPa.

Effect of the Inlet flow Velocity

The experiment was conducted to check the effect of the inlet flow on the rejection of solutes and permeate flux. The results are shown in Figure 7. The permeate flux increased from 1.4×10^{-5} to 1.9×10^{-5} m^3 m^{-2} s^{-1} as the inlet flow varied from 75 to 150 mL/min. The increase in the flux was about 20% compared to the initial flux. The permeate flux remained constant

Table IV. Simulation Results

Parameter	Notation	Experimental value	Predicted value	Error (%)
Steady-state permeate flux	$J_{p,ss}$	1.86×10^{5}	1.94×10^{-5}	4.2
Concentration of Pb(II) in the permeate	C_{p1}	2.61×10^{-3}	2.73×10^{-3}	4.8
Concentration of Cr(III) in the permeate	C_{p2}	0.87×10^{-3}	0.93×10^{-3}	6.0
Concentration of CB in the permeate	C_{p3}	4.36×10^{-3}	4.82×10^{-3}	9.5
Concentration of SDS in the permeate	C_{p4}	264.5×10^{-3}	278.7×10^{-3}	5.1
Concentration of TW80 in the permeate	C_{p5}	561.0×10^{-3}	592.0×10^{-3}	5.2

with further increases in the inlet flow. This was because of the increase in the cross-flow velocity on the membrane surface, which minimized the gel layer thickness. Up to 150 mL/min, the gel layer was eradicated to its minimum level, and further eradication was not possible. Hence, there was no increase in the permeate flux above a 150 mL/min flow rate. The rejections of CB, Cr, and Pb were found to be constant at 98, 98.5, and 99%, respectively. These results were in agreement with Vibhandik and Marathe.[28] The inlet flow was optimized at 150 mL/min.

Parametric Evaluation for a Continuous System

The steady-state ultrafiltration experiment was done under optimum operating conditions, namely, TMP = 100 kPa, $\alpha = 0.5$, S/M ratio = 10, and inlet velocity = 150 mL/min. The permeate and retentate streams were recycled to the feed tank to ensure that the initial feed concentration was constant. The results are depicted in Figure 8. The rejections of SDS, TW80, and CB were 90, 96, and 98.5%, respectively, whereas there was increase in the rejections of Cr and Pb as the time was varied from 5 to 15 min. The rejection of Cr increased from 75 to 96%, whereas the Pb rejection increased from 78 to 98% when the time was varied from 5 to 15 min. This increase in rejection may have been due to the formation of the gel layer, which offered resistance to the flow and indicated a decline in the permeate flux. As shown in the figure, we concluded that the equilibration time for the process was 12 min.

Validation of the Mathematical Model

An attempt was made to validate experimental data of the steady-state process with a mathematical model. Detailed theory of the mathematical model is depicted in a previous section. The application of a multiple-solute model was proposed by Manchalwar *et al.*[23] was tried to validate it with experimental data. The experiments were carried out at TMP = 100 kPa and optimized inlet feed velocity = 150 mL/min; the corresponding v was 0.001162 m/s. Equation (7) was solved with the Levenberg–Marqdaut method with a Gauss–Newton algorithm. $\Delta\pi$ and P_m were calculated by the solution of eqs. (8) and (9), respectively. We found that the $\Delta\pi$ value was 82 kPa. The membrane parameters, including k_i and K_{bi} were determined, as explained earlier.

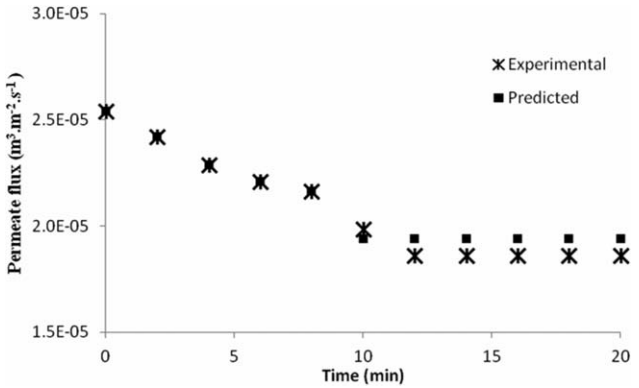

Figure 9. Comparison between the experimental and predicted permeate flux values.

$J_{p,ss}$ and the solute concentrations in the permeate were predicted at $\Delta P = 100{,}000$ N/m^2 and $v = 0.001162$ m/s by the multiple-solute model. The initial feed condition and the calculated membrane parameters are depicted in Tables II and III, respectively. With data from Tables I and II, models 7, 8, 9, and 10 were solved simultaneously with the algorithm given in Figure 2. The results are shown in Table IV.

As shown in Table IV, the metal-ion concentration was found to be in good agreement with the experimental data. The TW80 and SDS permeate concentrations showed a 5% departure from the experimental findings, and the CB permeate concentration value determined by the simulation shows a 9% relative error compared to the experimental value. According to Figure 9, the equilibration time for flux by prediction was 10 min; this was in good agreement with the experimental findings (12 min).

CONCLUSIONS

MEUF is a feasible process for simultaneously separating heavy-metal ions and organics from wastewater. The optimum parameters were as follows: S/M molar ratio = 10, $\alpha = 0.5$, TMP = 100 kPa, and inlet flow rate = 150 mL/min. There was about a 27% decrease in the permeate flux with the addition of TW80. The rejection of surfactants was increased because of CB, and there was a decrease in the metal-ion rejection. In the steady state, the rejection of metal ions increased from 5 to 15 min because of the formation of the gel layer. $J_{p,ss}$ was obtained as 1.86×10^{-5} m^3 m^{-2} s^{-1}. The multiple-solute model was applied to the experimental data. The solute concentration predicted by simulation showed a 4–9% relative error; this was in the acceptable range. The equilibration time was 10 min by simulation and was is in close agreement with the experimental value.

REFERENCES

1. Wahaab, R. A. *Bull. Environ. Contam. Toxicol.* **2001**, *66*, 770.
2. Dong, Y. *J. Environ. Manage.* **2011**, *92*, 408.

3. Baker, R. *Membrane Technology and Applications;* 2nd edition, John wiley and Sons LTD., England, **2004**.
4. Cheryan, M. Ultrafiltration and Microfiltration Handbook; CRC: Boca Raton, FL, **1988**.
5. Huang, Y.; Batchelor, B.; Koseoglu, S. S. *Sep. Purif. Technol.* **1994**, *29*, 1979.
6. Rosen, M. J. Surfactants and Interfacial Phenomena; Wiley: Hoboken, NJ, **2004**.
7. Huang, J.; Zeng, G.; Fang, Y.; Qu, Y.; Li, X. *J. Membr. Sci.* **2009**, *326*, 303.
8. Aoudia, M.; Allal, N.; Djennet, A.; Toumi, L. *J. Membr. Sci.* **2003**, *217*, 181.
9. Huang, J.; Peng, L.; Zeng, G.; Li, X.; Zhao, Y.; Liu, L.; Li, F.; Chai, Q. *Sep. Purif. Technol.* **2014**, *125*, 83.
10. Lee, J.; Yang, J.-S.; Kim, H.-J.; Baek, K.; Yang, J.-W. *Desalination* **2005**, *184*, 395.
11. Li, X.; Zeng, G.-M.; Huang, J.-H.; Zhang, D.-M.; Shi, L.-J.; He, S.-B.; Ruan, M. *Desalination* **2011**, *276*, 136.
12. Yenphan, P.; Chanachai, A.; Jiraratananon, R. *Desalination* **2010**, *253*, 30.
13. Zhao, B.; Xu, J.; Li, W.; Wang, H.; Che, H. *Asian J. Chem.* **2011**, *23*, 1509.
14. Vincent-Vela, M.-C.; Cuartas-Uribe, B.; Álvarez-Blanco, S.; Lora-García, J. *Desalination* **2012**, *284*, 14.
15. Tansel, B.; Bao, W. Y.; Tansel, I. N. *Desalination* **2000**, *129*, 7.
16. KrishnaKumar, N. S.; Yea, M. K.; Cheryan, M. *J. Membr. Sci.* **2004**, *244*, 235.
17. Mohammadi, T.; Kohpeyma, A.; Sadrzadeh, M. *Desalination* **2005**, *184*, 367.
18. Ghaffour, N. *Desalination* **2004**, *167*, 281.
19. Damaka, K.; Ayadi, A.; Zeghmatib, B.; Schmitz, P. *Desalination* **2004**, *161*, 67.
20. Katsikaris, K.; Boukouvalas, C.; Magoulas, K. *Desalination* **2005**, *171*, 1.
21. Ahmad, A. L.; Chong, M. F.; Bhatia, S. *Chem. Eng. Sci.* **2006**, *61*, 5057.
22. Chitikela, S.; Dentel, S. K.; Allen, H. E. *Analyst* **1995**, *120*, 2001.
23. Manchalwar, S. M.; Anthati, V. A.; Marathe, K. V. *J. Hazard. Mater.* **2010**, *184*, 485.
24. Dong, J. H.; Shi, M. Y. *J. Membr. Sci.* **2004**, *241*, 335.
25. Karode, S. K. *J. Membr. Sci.* **2001**, *188*, 9.
26. Chapra, S. C.; Canale, R. P. Numerical Methods for Engineers; McGraw-Hill: New York., **1998**.
27. Fang, Y.-Y.; Zeng, G.-M.; Huang, J.-H.; Liu, J.-X.; Xu, X.-M.; Xu, K.; Qu, Y.-H *J. Membr. Sci.* **2008**, *320*, 514.
28. Vibhandik, A. D.; Marathe, K. V. *Frontiers Chem. Sci. Eng.* **2014**, *8*, 79.
29. Wijmans, J. G.; Nakao, S.; Smolders, C. A. *J. Membr. Sci.* **1984**, *20*, 115.